Laboratory Investigation (2019) 99:1714–1727
https://doi.org/10.1038/s41374-018-0180-y

ARTICLE

Lens-specific conditional knockout of *Msx2* in mice leads to ocular anterior segment dysgenesis via activation of a calcium signaling pathway

Wenting Yu[1] · Ziyan Yu[1] · Danhong Wu[2] · Jiao Zhang[1] · Ying Zhu[1] · Yang Zhang[3] · Hong Ning[3] · Mingwu Wang[4] · Jinsong Zhang[1] · Jiangyue Zhao[1]

Received: 2 December 2017 / Revised: 25 October 2018 / Accepted: 16 November 2018 / Published online: 25 January 2019

Abstract

Ocular anterior segment dysgenesis (ASD) is a failure of normal development of anterior structures of the eye, leading to lens opacification. The underlying mechanisms relating to ASD are still unclear. Previous studies have implicated transcriptional factor muscle segment homeobox 2 (*Msx2*) in ASD. In this study, we used *Msx2* conditional knockout (CKO) mice as a model and found that *Msx2* deficiency in surface ectoderm induced ASD. Loss of *Msx2* function specifically affected lens development, while other eye structures were not significantly affected. Multiple lines of evidence show that calcium signaling pathways are involved in this pathogenesis. Our study demonstrates that *Msx2* plays an essential role in lens development by activating a yet undetermined calcium signaling pathway.

Introduction

Ocular anterior segment dysgenesis (ASD) describes a spectrum of clinically and genetically heterogeneous congenital disorders affecting anterior structures including the cornea, iris, lens, ciliary body and ocular drainage structures that often lead to impaired vision. Clinical manifestations of ASD are variable and include corneal opacities, cataracts, iris hypoplasia and iridocorneal adhesions. In addition, ASD is associated with extraocular defects [1]. ASD is a multigenic disorder [2], including mutations in several genes such as *Cyp1b1, Foxc1, Foxc2, Foxe3, Lmx1b, Maf, Pax6, Pitx2*, and *Pitx3* [3]. Many of these genes encode transcription factors responsible for development and maturation of cornea and lens [4] . Although these genes have long been recognized in the etiology of ASD, the underlying mechanism remains elusive.

Ocular anterior segment development involves a series of highly orchestrated and complex inductive interactions between tissues derived from different embryonic lineages: the surface ectoderm, neural ectoderm, neural crest and cranial paraxial mesoderm [5, 6]. It is well known that homeobox genes function as essential transcriptional regulators in a variety of developmental processes [7]. *Msh* homeobox genes are defined as a group of highly conserved homeodomain proteins that generally function as transcriptional repressors, are expressed at epithelial-mesenchymal transition sites during embryogenesis and are responsible for the development of skull, hair follicles, teeth, heart and brain. The murine *Msx* family is comprised of 3 members, *Msx1*, *Msx2*, and *Msx3*. *Msx3* is absent in the human genome [8–12]. *Msx2* acts as an upstream regulator in optic vesicle development [13–15]. In our previous study, *Msx2* traditional knockout was linked to Peter's anomaly (a subtype of ASD) and severe microphthalmia, which further substantiates its role in controlling eye development [14, 15]. Changes in *FoxE3* and *Prox1* expression support

These authors contributed equally: Wenting Yu, Ziyan Yu

Supplementary information The online version of this article (https://doi.org/10.1038/s41374-018-0180-y) contains supplementary material, which is available to authorized users.

✉ Jiangyue Zhao
jyzhao@cmu.edu.cn

[1] Department of Ophthalmology, The Fourth Affiliated Hospital, China Medical University, 110005 Shenyang, China

[2] Department of Neurology, Shanghai Fifth People's Hospital, Fudan University, 200240 Shanghai, China

[3] Department of Ophthalmology, The First Affiliated Hospital, China Medical University, 110001 Shenyang, China

[4] Department of Ophthalmology, University of Arizona College of Medicine, Tucson, AZ 85711, USA

the importance of *Msx2* in controlling transcription of target genes critical for early eye development [14]. During eye development, *Msx2* transcripts first appear in the optic vesicle (OV) and adjacent ectoderm at E9.5. Along with lens genesis, *Msx2* transcripts are located in the lens epithelial cells at E10.5 and E11.5 and then expressed in differentiated lens fiber cells after E12.5 [15]. The decrease of *Msx2* expression hinders normal surface ectoderm development through several signaling pathways. Further investigation into these complex interactions among *Msx2*, various transcriptional regulators and signaling molecules may help clarify the pathogenesis of ASD and other congenital eye diseases.

The limitation of our previous study is that *Msx2* was knocked out in both surface ectoderm and neuro ectoderm. Microphthalmia and retina malformation were found in *Msx2* traditional knockout mice. Moreover, it is hard to rule out the effect of retina-lens sequential induction during eye development, which could lead to misinterpretation of the *Msx2* gene function in ocular development. Conditional gene knockout is a technique used to eliminate a specific gene in a specific tissue. The conditional gene knockout technique may eliminate many of the undesired effects induced by traditional gene knockout. Thus, in our present study, we used head surface ectoderm-specific *Msx2* gene knockout mice as a model and found that *Msx2* deficiency leads to ASD without cornea-lentoid adhesions. Loss of *Msx2* in the surface ectoderm down-regulated Gja8 and crystallin expression and up-regulated Tgm2, Capn1, and Camk2b expression in mouse lens. *Msx2* therefore acts as an upstream gene of a calcium signaling pathway in ocular development.

Material and methods

Mice

All animal experiments were performed in accordance with approved guidelines and regulations established by the China Medical University (16005 M). We conducted the studies according to the guidelines provided by the Care and Use of Laboratory Animals of China Medical University according the Chinese version of 8th Guide (http://202.118.40.32/sydwb/info/1834/1177.htm) which followed the US Public Health Management Policy. The mice used in this study were housed in the controlled specific-pathogen-free (SPF) environment and cared for according to the approved protocol. Mice used in the experiments were crested on the BALB/c, C57/B6 and FVB background and kept under C57/B6 background [16]. A previous study demonstrated that after *Le-Cre*$^{+/-}$ was backcrossed to CBA/Ca for seven generations, some *Le-Cre*$^{+/-}$; *Pax6*$^{+/+}$, as well as *Le-Cre*$^{+/-}$; *Pax6*$^{fl/+}$ mice exhibited significant eye abnormalities; and after 2 generations of backcrossing *Le-Cre*$^{+/-}$ mice to the original FVB/N strain, eye abnormalities in *Le-Cre*$^{+/-}$; *Pax6*$^{+/+}$ mice were diminished [17]. However, in our study, no eye abnormalities were found in the 15th generations of *Le Cre*$^{+/-}$; *Msx2* $^{fl/fl}$; and *Le Cre*$^{+/-}$; *Msx2* $^{fl/+}$ mice, which is shown in Supplementary Fig. 1. To address whether *Msx2* function in lens development is intrinsic to local *Msx2* function, we generated *Msx2* conditional knockout mice (*Msx2* CKO) by crossing *Msx2* floxed mice with *Le-Cre* mice, whose Cre-recombinase expression is regulated by *Pax6-Le* tissue-specific regulatory elementals which is only active in surface ectoderm, as reported previously [18]. The experimental mice were genotyped by tail polymerase chain reaction (PCR). The *Le-Cre* heterozygous mice were bred with mice carrying floxed *Msx2* alleles (*Msx2* $^{flox/flox}$). The male mice carrying *Le-Cre;Msx2*$^{flox/+}$ were subsequently crossed with females carrying *Msx2*$^{flox/flox}$ to generate *Le-Cre; Msx2*$^{flox/flox}$ (*Msx2* CKO) mice. Littermates were used as the experimental group and littermates carrying *Msx2*$^{flox/flox}$ (*Msx2* control) were served as controls. *Msx2* heterozygous transgene mice were not used as the control group. PCR primers for *Le-Cre* genotyping are as follows: *Le-Cre* (forward), 5′-TAATCGCCATCTTCCAGCAG-3′, *Le-Cre* (reverse), 5′-CTCTGGTGTAGCTGATGATC-3′; forward, 5′-GTTGAGC CGAGTCTCCCACCT-3′ and reverse 5′-GATTCCTTGGG CGGCTTCTT-3′) for floxed alleles of *Msx2*.

Histological preparation of mice embryos and eyeballs

Pregnant female mice were sacrificed at various time points after conception. The mice were anesthetized by sevoflurane and then sacrificed by cervical dislocation before the procurement of their embryos or eyeballs. The embryos and eyeballs were fixed in 4% paraformaldehyde overnight at 4 °C, then dehydrated through graded alcohol, cleared in xylene, and embedded in paraffin. Sections were cut to 4 μm and stained with hematoxylin and eosin. Sections were photographed using an Olympus microscope (BX51, Olympus, Japan) with a SPOT camera. Three mice/six eyes from each group were evaluated to compare eye structures between these two groups and the experiment was repeated three times.

Lens measurement

Electronic balance (Acculab ALC, Germany) was used to measure mice lens quality. After obtaining mice lenses, the residual surface water was removed and the lens were placed in the same EP tube carefully for testing. Six mice/12 lenses from each group were evaluated to compare the lens wet weight of these two groups and was repeated three times.

Table 1 List of primers used for real-time quantitative PCR

Gene	Forward primer (5'–3')	Reverse primers (5'–3')
Capn1	AGTGGAAAGGACCCTGGAGT	CCGGTGTAAGGTTGCAGATT
Tgm2	CACCTGAACAAACTGGCAGA	CAGGGTCAGGTTGATGTCCT
Camk2b	GGGACACCGTTACTCCTGAA	TTGAGCTTCCTCCTTGCATT
Gja8	GAAAGGACCGTGAAGCTGAG	AGGATGCGGAAACCATACAG
Cryab	TTCTTCGGAGAGCACCTGTT	TGCTTCACGTCCAGATTCAC
Cryba1	CTTCTGTGGGCAACAGTTCA	CCACTGGCGTCCAATAAAGT
Crybb1	CTTTGAGCAATCTGCCTTCC	CACGGTCACAGAAGCCATAA
Crybb3	GACAGCCTGTTGGAGAAGGT	GGAGGGACAGGAGAATGTCA

Whole-mount in situ hybridization

Embryos of various ages were fixed overnight in 4% paraformaldehyde in PBS. Whole-mount in situ hybridization was performed according to standard protocols [19]. The *Msx2* cDNA plasmid was purchased from ATCC (Manassas, VA) [18]. All RNA probes were labeled with digoxigenin-UTP according to the manufacturer's recommendations (Roche Applied Science). Three mice/6 lenses from each group were evaluated to compare *Msx2* mRNA expression between these two groups and the experiment was repeated times.

BrdU labeling and TUNEL assay

Pregnant mice were sacrificed at various time points after conception. One hour before sacrificing, the mice were injected intraperitoneally with 100 µg BrdU (Sigma, St. Louis, USA) per gram of body weight. For post-natal mice, BrdU was injected intraperitoneally 2 h before sacrifice [20]. Then the embryos were put into ice-cold PBS.

Apoptotic cells were detected by using the fluorescein in situ Cell Death Detection Kit (Roche Applied Science, Indianapolis, IN). Briefly, 4% PFA-fixed tissue sections were treated with Proteinase K (20 µg/ml) for 20 min. Fragmented DNA was labeled with fluorescein-dUTP, then cell nuclei were counterstained with DAPI. Histological photos were taken by Olympus fluorescence microscope equipped with a Spot CCD camera. Three mice/six lenses from each group were evaluated to detect lens cell proliferation and apoptosis in each of the two groups and the experiment was repeated three times.

RNA-seq analysis and quantitative PCR

Lens RNA was extracted from *Msx2* control and *Msx2* CKO mice at P60 using RNAeasy™ micro kit (R0024, Beyotime, China). RNA purity was checked using the Nanophotometer spectrophotometer (IMPLEN, CA, USA). RNA concentration was measured using Qubit RNA Assay kit in Qubit 2.0 flurometer (Life Technologies, CA, USA), and RNA integrity was assessed using the RNA nano 6000 Assay kit of the Bioanalyzer 2100 system (Agilent Technologies, CA, USA). The RNA-seq was carried out by Illumina HiSeq sequencing (Novogene Bioinformatics Institute, Beijing, China). Differential expression analysis: prior to differential gene expression analysis, for each sequenced library, the read counts were adjusted by edgeR program package through one scaling normalized factor. Differential expression analysis of two conditions was performed using the edgeR package (3.12.1). The *P* values were adjusted using the Benjamini and Hochberg method. Corrected *P*-value of 0.05 and absolute fold change of 2 were set as the threshold for significantly differential expression. Gene Ontology (GO) enrichment analysis of differentially expressed genes was implemented by the clusterProfiler R package, in which gene length bias was corrected. GO terms with corrected *P* value less than 0.05 were considered significantly enriched by differential expressed genes. KEGG is a database resource for understanding high-level functions and utilities of the biological system, such as the cell, the organism and the ecosystem, from molecular-level information, especially large-scale molecular datasets generated by genome sequencing and other high-through put experimental technologies (http://www.genome.jp/kegg/). We used clusterProfiler R package to test the statistical enrichment of differential expression genes in KEGG pathways.

Quantitative PCR (qPCR) was used to verify the results by using SYBR Premix Ex TaqTM II kit (Takara, China) and analyzed based on the equation $RQ = 2^{-\Delta\Delta CT}$. The sequences of real-time qPCR primers were listed in Table 1. Ten mice/20 lenses at P60 from each group were evaluated to compare gene expression and the experiment was repeated three times.

Immunofluorescence and immunohistochemistry

After deparaffinization and rehydration, the sections were boiled for 10 min in diluted with ddH_2O from ×100 to ×1 antigen repair solution (MXB Biotechnologies, China) and blocked with 5% BSA for 1 h. Anti-Capn1 monoclonal

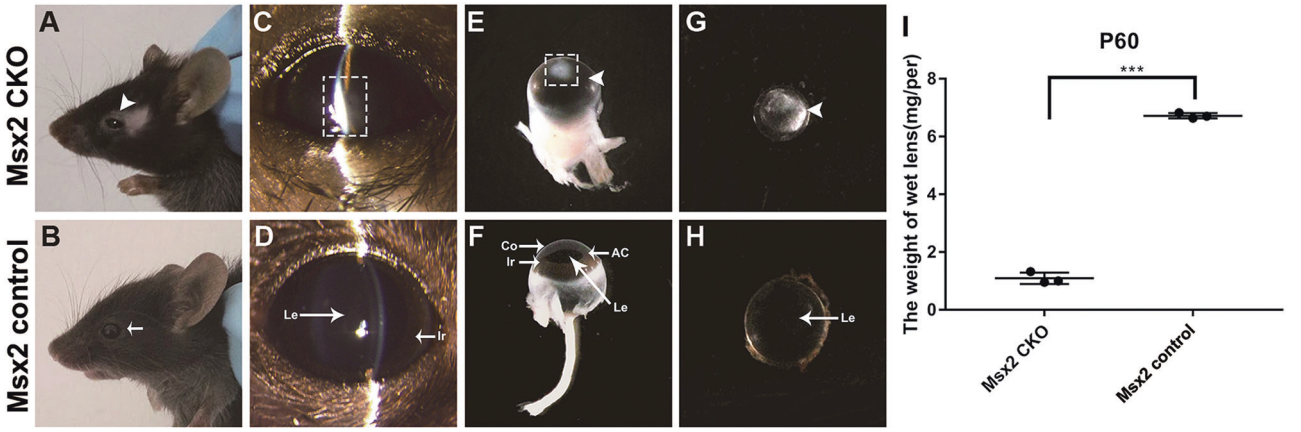

Fig. 1 Generation of surface ectoderm-specific conditional *Msx2* knockout mouse. **A–H** Representative *Msx2* CKO and *Msx2* control mice eyes at postnatal-day-60. (**A** vs. **B**). Gross examination of *Msx2* CKO (arrow) and control eyes (arrowhead). Eye socket depression, small eye, lack of eyelashes and narrow palpebral fissure were seen in *Msx2* CKO mice **A**. **C** vs. **D** *Msx2* CKO mice indicated corneal opacities, iris cornea synechia (virtual box) was found in *Msx2* CKO mice by slit lamp under mydriatic conditions but not in in *Msx2* control mice. **E** vs. **F** There was cornea stroma thickening; cornea-iris adhesion (virtual box); and the anterior chamber was absent (arrowhead) in *Msx2* CKO mice but not in in *Msx2* control mice. **G** vs. **H** A small irregular shaped lens and lens opacity (arrowhead) were found in *Msx2* CKO mice but not in in *Msx2* control mice (arrow). Three mice/six eyes from each group were evaluated to compare general phenotype of these two groups; $N = 3$; Co cornea, Le lens, Ir iris, AC anterior chamber (cavity between posterior cornea, iris, lens). **I** Lens wet weight of *Msx2* CKO was much less than *Msx2* control mice at P60. Six mice/12 lenses from each group were evaluated to compare the wet weights; $N = 3$; $^{***}P < 0.0001$

antibody (ab108400, ABCAM, USA, 1:100), Anti-Tgm2 polyclonal antibody (ab421, ABCAM, USA, 1:500), Anti-Camk2b polyclonal antibody (ab34703, ABCAM, USA, 1:200), Anti-Gja8 polyclonal antibody (ab222885, ABCAM, USA, 1:100); Anti-Cryab polyclonal antibody (ab5577, ABCAM, USA, 1:200), anti-Cryba1 polyclonal antibody (PA5-71690, ThermoFisher Scientific, USA, 1:500), anti-Crybb1 polyclonal antibody (bs-12582R, Bioss Antibodies, China, 1:500), and anti-Crybb3 polyclonal antibody (21009-1-AP, Proteintech Systems, USA, 1:100) were used as primary antibody. Anti-Rabbit antibody488 (A-21206, Invitrogen, USA), and anti-Rabbit antibody594 (A-21207, Invitrogen, USA) as secondary antibodies were incubated at room temperature for 2 h. Cell nuclei were counterstained with DAPI. DAB (TA-060-QHDX ThermoFisher Scientific, USA) was used for color development followed by hematoxylin counterstaining in immunohistochemistry assay. Three mice/six lenses from each group were evaluated to compare these proteins expression of these two groups and repeated 3 times.

Statistical analysis

Data were recorded as mean ± standard deviation (SD), and analyzed using SPSS for Windows, version 16.0 (SPSS Inc. IL, USA). Significant difference was evaluated by analysis of unpaired Student's-test (two-tailed). Statistical significance was defined as indicated in the figure legends.

Results

Targeted disruption of *Msx2* on eye surface ectoderm led to ASD

Our previous study using *Msx2* germline knockout mice as an experimental model showed that loss of *Msx2* can affect eye development [14]. In this study, *Msx2* was conditionally deleted using *Le-Cre* to analyze its function in lens development. Morphological analysis revealed abnormal eye development characterized by eye socket depression, small eye, lack of eyelashes and narrow palpebral fissure in *Msx2* CKO mice (Fig. 1A) but not in *Msx2* control mice (*Msx2* floxed only; Fig. 1B) and *Le-Cre* heterozygous transgene mice (Fig S1) at postnatal day 60 (P60). Moreover, corneal opacities, iris cornea synechia (virtual box) were found in *Msx2* CKO mice by slit lamp under mydriatic condition but not in in *Msx2* control mice (Fig. 1C vs. D) and *Le-Cre* heterogenous transgene mice (Fig S1). Furthermore, cornea stroma thickening; cornea-iris adhesion (virtual box) and disappearance of the anterior chamber (arrowhead) were found in *Msx2* CKO mice but not in in *Msx2* control mice (Fig. 1E vs. F). Small irregularly shaped lenses and lens opacity (arrowhead) were found in *Msx2* CKO mice but not in in *Msx2* control mice (Fig. 1G vs. H), which are the typical phenotypes observed in human ASD. To more precisely quantify the abnormality of lens development induced by *Msx2* CKO, lens wet weight was compared between *Msx2* CKO and control mice at P60. Lenses were

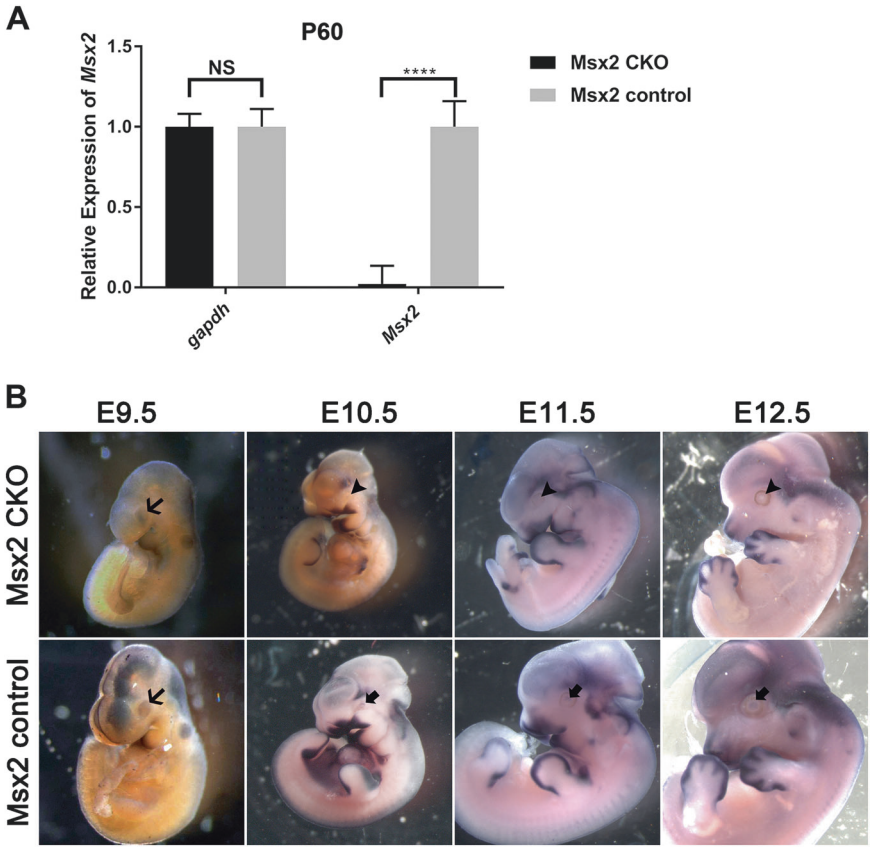

Fig. 2 Verification of Msx2 deficiency in *Msx2* CKO mice. **A** RT-qPCR quantification of *Msx2* mRNA of *Msx2* CKO and control mice lens at postnatal-day-60. *gapdh* serves as a loading control. *Msx2* CKO is normalized to *Msx2* control which was arbitrarily set as 1. *Msx2* mRNA expression iswas absence in *Msx2* CKO compared to *Msx2* control group. Ten mice/20 eyes from each group were evaluated to compare Msx2 expression; $N = 3$; ****$P < 0.00001$. **B** Whole mount in situ hybridization shows that *Msx2* mRNA transcripts were not detectable in *Msx2* CKO at E9.5 optic vesicle (arrow) and absence of *Msx2* mRNA in the *Msx2* CKO lens vesicle (arrowhead) compared to *Msx2* control group (arrow) at E10.5, E11.5, and E12.5. Three mice/6 eyes from each group were evaluated to compare *Msx2* mRNA; $N = 3$

significantly smaller in *Msx2* CKO mice (1.09 ± 0.11) compared with *Msx2* control (6.72 ± 0.05) (Fig. 1I), further confirming the abnormal development of lens after loss of *Msx2* function.

Conditional *Msx2* knockout specifically affected lens development

To confirm that *Msx2* gene conditional disruption can specifically delete *Msx2* gene expression in lens, we first isolated total RNA from P60 mice lens and analyzed *Msx2* mRNA level by RT-qPCR. Our data show a significant difference in *Msx2* mRNA expression level between *Msx2* CKO and control mice (Fig. 2A). From E9 to E9.5, Pax6 protein was eliminated in the Le-mutant surface ectoderm (SE) [15], and from E10.5 it was undetectable [15, 17]. Our whole-mount in situ hybridization results showed identical results. *Msx2* mRNA transcripts in *Msx2* CKO at E9.5 optic vesicle (arrow). However, transcripts were seen in the developing lens vesicle from E10.5 to E12.5 in the *Msx2* control group (arrow), but was not found in *Msx2* CKOs (arrowhead) (Fig. 2B). These results confirmed that the tissue specificity of conditional *Msx2* knockout.

Next, we compared the phenotype induced by traditional *Msx2* knockout mice (*Msx2* KO) and *Msx2* CKO at E14.5 and P60 . Consistent with our previous findings [14], *Msx2* KO eyes possessed defective lenses (Fig. 3C arrow). The eye phenotype of *Msx2* CKO was less severe than that of *Msx2* KO mice at E14.5 (Fig. 3B vs. C). *Msx2* KO mice at E14.5 demonstrated much smaller eyes with thickened retina. (Fig. 3D). In contrast, *Msx2* CKO mice at E14.5 displayed slightly thickened retina, but much less severe than the *Msx2* KO (Fig. 3E vs. F). Smaller lenses with thickened retina (arrowhead) and abnormally proliferating primary vitreous (arrow) were observed in *Msx2 KO* mice at E14.5 (Fig. 3F). Smaller lens, uneven thickness and detached retina were detected in *Msx2* CKO and *Msx2* KO mice at P60, compared with the *Msx2* control group (Fig. 3H, I vs. G). Retinal folds and detachment were observed in *Msx2* KO retina at P60 (Fig. 3I). Therefore, it appears that *Msx2* CKO specifically disrupts lens development while minimally affects other eye structures; this is most apparent at E14.5.

Abnormal lens development in *Msx2* CKO mice at early embryonic stages

Next, we systemically investigated *Msx2* CKO mice lens development by gross examination and histological analysis of *Msx2* CKO mice lens at different embryonic development stages. Subtle changes in the eyes of the *Msx2* CKO mice were first detected as early as E12.5, compared with

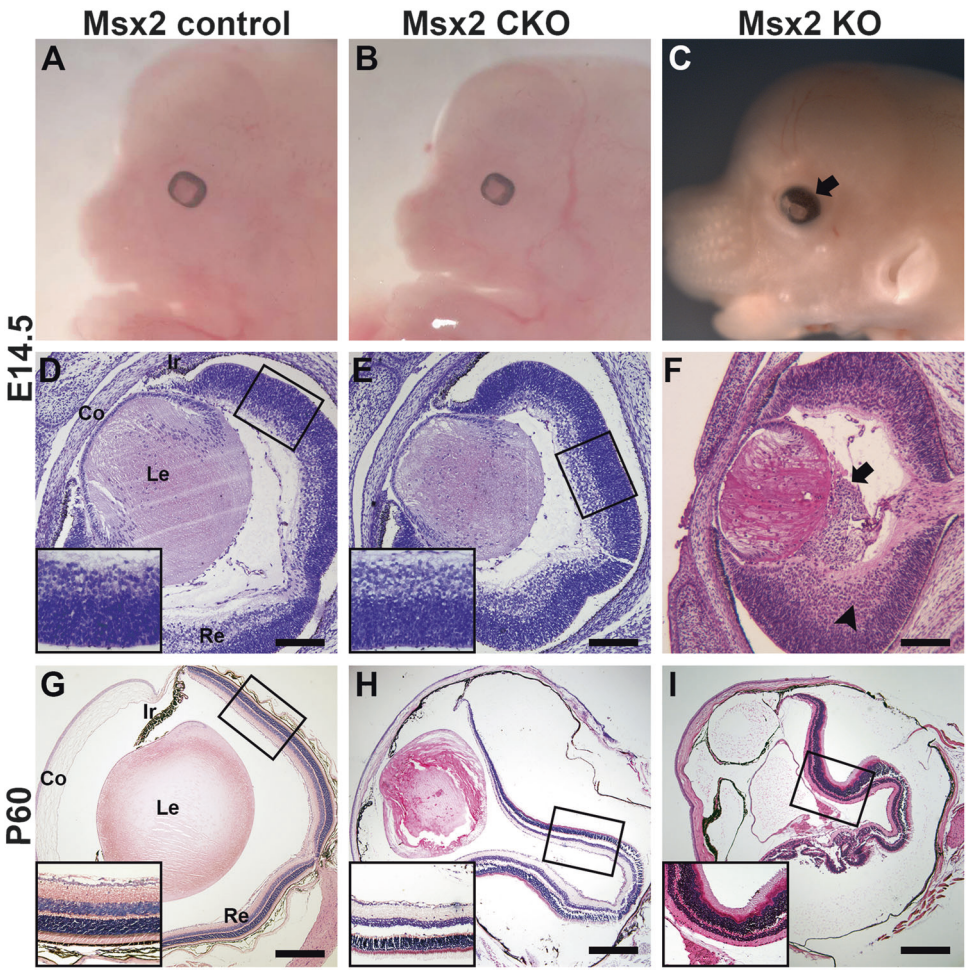

Fig. 3 *Msx2* CKO mice showed defective lens only, while the entire eye was abnormal in KO mice. Lens morphology and histology of *Msx2* control, *Msx2* CKO and *Msx2* KO mice at E14.5 and P60. **A–C** Phenotypes of *Msx2* CKO mice, *Msx2* KO mice and control mice. Whole mount embryo of *Msx2 CKO* mice show a slightly smaller eye (**B**). *Msx2* KO mice with much smaller eyes and severe ocular abnormality (arrow) (**C**). **D–F** Histology analysis of ocular development at E14.5 of *Msx2* CKO mice, *Msx2* KO mice and control mice. *Msx2* CKO mice at E14.5 stage displayed a little bit thickened retina but much less severe than *Msx2* KO (**E** vs. **F**). Bottom panels showed the enlarged view of the boxed regions (**D–E**). Smaller lenses with thickened retina (arrowhead) and abnormally proliferated primary vitreous (arrow) wascould be observed in *Msx2 KO* mice (**F**). Small lenses were seen in *Msx2 CKO* mousee eyes (**E**). **G–I** Histology analysis of control mice, *Msx2* CKO and *Msx2* KO mice eyes at postnatal-day-60. Smaller lens, uneven thickness and detached retina detected in *Msx2* CKO and *Msx2 KO* mice at P60 compared with *Msx2* controls (**H**, **I** vs. **G**). Retinal folds and detachment were observed in *Msx2* KO retina at P60 (**I**). Bottom panels showed an enlarged view of the boxed regions (**G–I**). Three mice/six eyes from each group were evaluated to compare eye structures; $N = 3$; Co cornea; Le lens; Ir iris, Re retnia; Scale bars: 100 um (**D–F**), 200 um (**G–I**)

littermate controls (Fig. 4A, B). Examination of histologic sections revealed that the lens of the *Msx2* CKO mice appeared to be smaller but completely developed from E12.5 to E18.5 (Fig. 4A, B). After delivery, abnormal development of eyes in the mutants could be easily recognized as the anterior expansion of the iris pigmented epithelium. Smaller lens and forward movement of lens were found from P2 (Fig. 4A, B). In severe case, lens and cornea adhesion was found after delivery. The severity of lens and cornea defects in the eyes of *Msx2* CKO mice varied among animals and even between eyes of the same animals.

In order to more clearly demonstrate lens defects caused by loss of *Msx2* function, lens size was quantified by measuring the anteroposterior and horizontal diameters in both groups from E12.5 to P8. A schematic diagram (Fig. 4C) shows the measurements of anteroposterior axis (D), rectilinear axis (E) and corneal thickness (F). There was statistically significant difference in anteroposterior diameter from E14.5 to P4 between these two groups (Fig. 4D). Similarly, horizontal diameter difference between *Msx2* control and CKO mice was also observed later, at E16.5 (Fig. 4E). We also examined and quantified the corneal thickness of mice from E12.5 to P8 and did not observe a statistical difference between the two groups before birth (data not shown). However, after birth, corneal thickness was significantly decreased in *Msx2* CKO mice

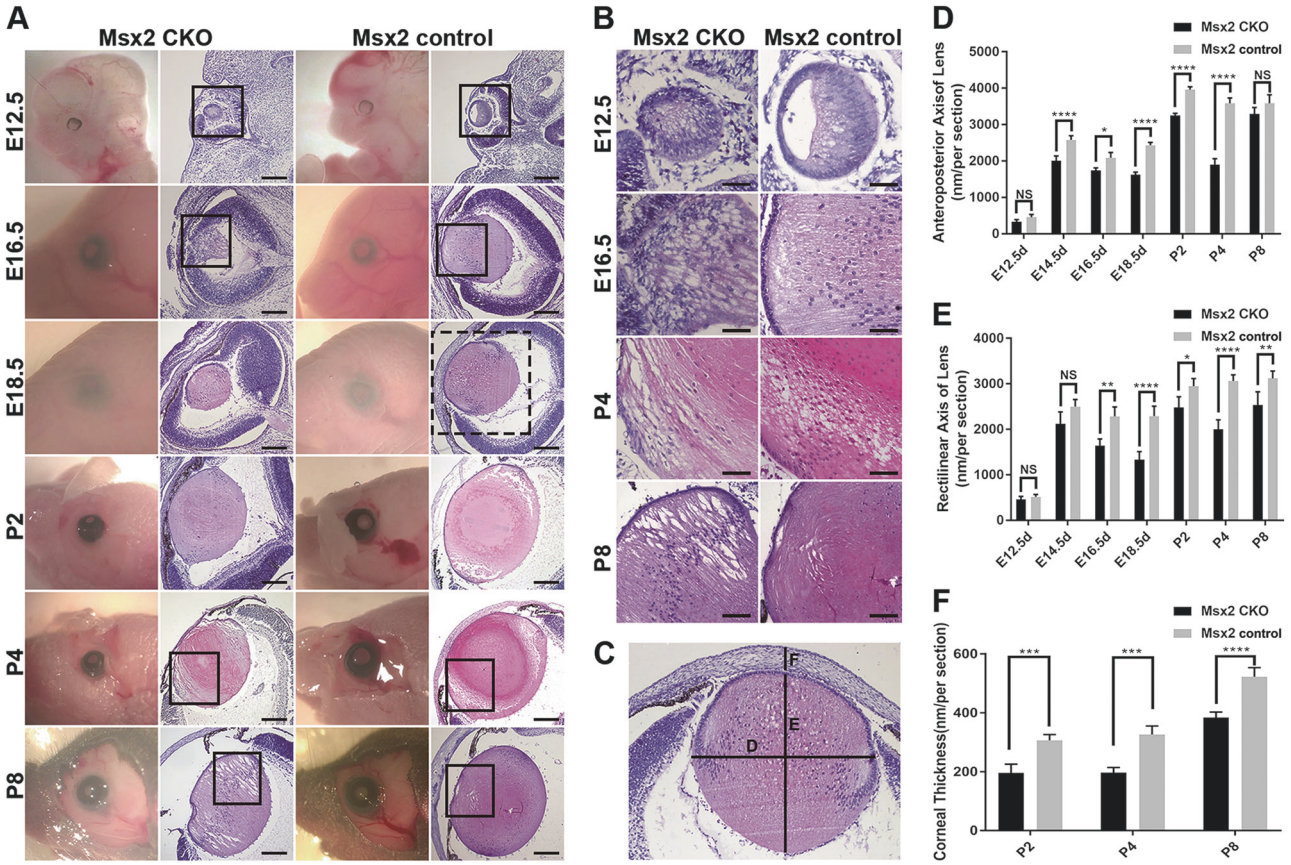

Fig. 4 Lens development in *Msx2* CKO prenatally and postnatally. **A** Morphological and histological analysis of eyes in *Msx2* CKO and control mice from E12.5 to P8. The boxed area is enlarged in **B**. **C** Schematic diagram showing how to measure anteroposterior axis (**D**), rectilinear axis (**E**) and corneal thickness (**F**). Measurement of anteroposterior axis and rectilinear axis of lens in *Msx2* CKO and control mice from E12.5 to P8 (**D–E**). $N = 3$; $^{*}P < 0.05$, $^{**}P < 0.001$, $^{***}P < 0.0001$, $^{****}P < 0.00001$. **F** Measurement of corneal thickness of *Msx2* CKO and control mice from P2 to P8. Three mice/six eyes from each group were evaluated to compare eye structures; $N = 3$; Scale bars: 100 um (**A**), 50 um (**B**); $^{***}P < 0.0001$

(Fig. 4F). In summary, *Msx2* CKO-induced aberrant lens development was observable at early embryonic stages.

Abnormal proliferation and apoptosis in *Msx2* CKO lens

In order to determine the phenotypes of the *Msx2* conditional knockout, lens cell proliferation and apoptosis were analyzed by immunofluorescence. BrdU positive cells (arrow in Fig. 5A) were observed at anterior lens epithelium cell as early as E12.5 in two groups. From E12.5 to E16.5, the percentage of BrdU-positive lens epithelial cells in both two groups was significantly increased (Fig. 5C). At E16.5, the number of BrdU positive lens epithelial cells was significantly reduced in *Msx2* CKO mice compared with *Msx2* control mice (Fig. 5A, C). From E16.5 to P8, the percentage of BrdU-positive lens epithelial cells in both two groups was decreased (Fig. 5C). The ratio of BrdU-positive cells at P8 between the two groups was virtually identical (Fig. 5C). The percentage of BrdU positive lens epithelial cells in *Msx2* CKO mice was significantly less than the control group, especially from E16.5 to P2 (Fig. 5A, C). *Msx2* CKO mice have fewer BrdU positive cells than *Msx2* control mice at each developmental stage (Fig. 5C). Lens cell apoptosis rates increased from E12.5 to E14.5 and then decreased with age until P8 in *Msx2* CKO mice (Fig. 5D). The apoptosis rate was significantly decreased in *Msx2* CKO mice at each stage compared with the control group. Few apoptotic lens cells were found in *Msx2* control mice from E12.5 to P8 (Fig. 5B, D). In contrast, *Msx2* CKO mice have more apoptotic lens cells at each stage (Fig. 5D). These results indicate that *Msx2* deficiency impairs lens development by suppressing cell proliferation and promoting cell apoptosis.

Variation of gene expression in *Msx2* conditional knockout lens

In order to gain a deeper understanding of how lens phenotypes result from conditional *Msx2* deletion, we

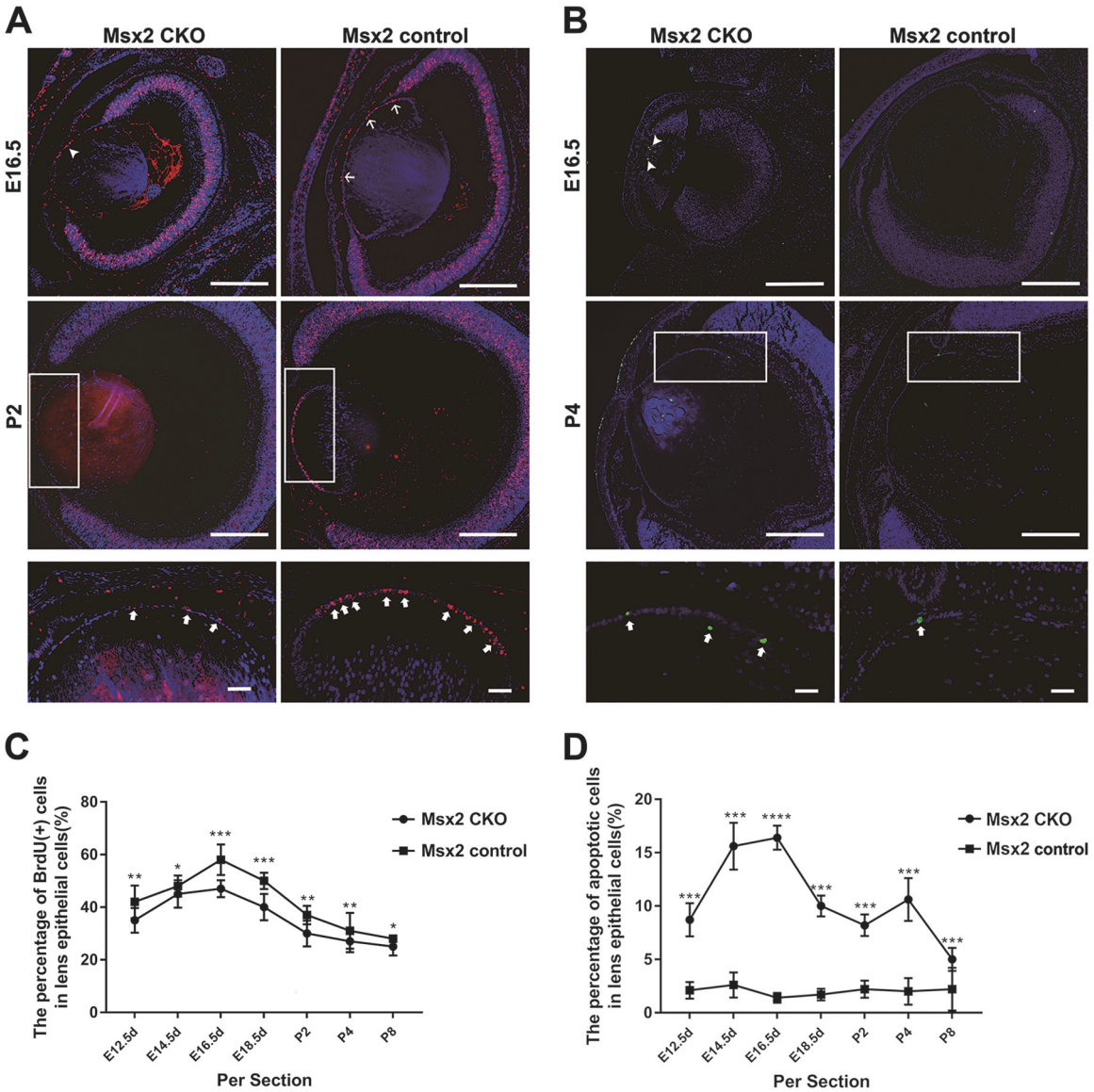

Fig. 5 Defective proliferation and enhanced apoptosis of lens in *Msx2* CKO mice. **A** BrdU staining of *Msx2* CKO and *Msx2* control mice eyes at E16.5 and P2. Arrows indicate the BrdU positive lens epithelial cells. Bottom panels show the enlarged view of the boxed regions in P2 panels. The percentage of BrdU positive lens epithelial cells is calculated in **C**. **B** Lens cell apoptosis was determined by TUNEL assay at E16.5 and P4. Arrows indicate the apoptotic lens epithelial cells. Bottom panels show the enlarged view of the boxed regions in P4 panels. The percentage of apoptosis cells is calculated in **D**. Three mice/six eyes from each group were evaluated to compare $BrdU^+$ staining and lens cell apoptosis; $N = 3$; Scale bars: 100 um; $^*P < 0.05$, $^{**}P < 0.001$, $^{***}P < 0.0001$

conducted RNA-seq analysis of lenses isolated from p60 *Msx2* CKO and *Msx2* control mice. The RNA-seq data and protocols have been submitted to NCBI's Gene Expression Omnibus (GEO) database with a GEO accession number of GSE114854. The volcano plot detected 1911 differentially expressed genes (DEGs) in *Msx2* CKO mice compared to the control mice. The selection of these 1911 genes was based on greater than 2-fold change in expression of genes between *Msx2* CKO and *Msx2* control mice. Among them, 1586 genes were upregulated (red) and the rest were downregulated (green) (Fig. 6A). Gene Ontology (GO), Kyoto Encyclopedia of Genes and Genomes (KEGG) Pathway and Reactome Pathway were applied to analyze differentially expressed mRNAs. GO enrichment analysis comprised 3 structured networks including biological processes (BP), cellular components (CC) and molecular function (MF). Among them, eye development in BP, ion channel complex in CC and ion channel activity, calcium ion binding and structural constituent of lens in MF closely regulate lens development (Fig. 6B) [21, 22]. Pathway analysis showed that 20 pathways were highly enriched among the abnormally expressed mRNAs (Fig. 6C). Among them, calcium signaling pathway was directly related to the lens opacification [23], ranking the fifth and associated with

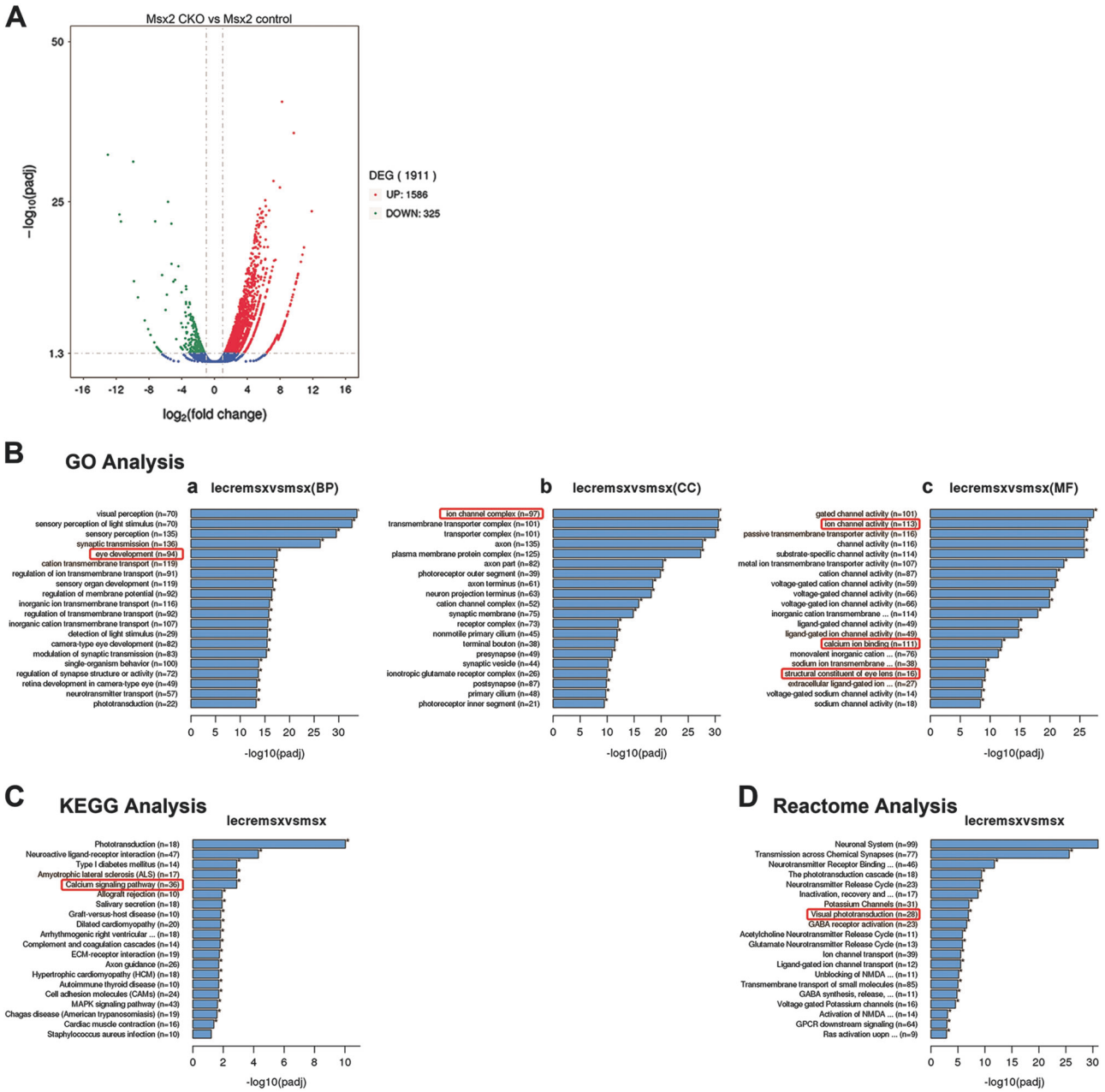

Fig. 6 RNA-seq analysis of *Msx2* CKO and *Msx2* control mice lens. **A** Volcano plot of RNA-Seq analysis of lens isolated from p60 *Msx2* CKO and *Msx2* control mice. The volcano plot detected 1911 differentially expressed genes (DEGs) in *Msx2* CKO mice compared to the control mice. Among them, 1586 genes were upregulated (red) and the rest were downregulated (green). **B–D** Gene Ontology (GO), Kyoto Encyclopedia of Genes and Genomes (KEGG) Pathway and Reactome Pathway were applied to analyze differentially expressed mRNAs. The red boxes highlighted the related pathways

36 DEGs. Reactome pathway analysis also confirmed that gene *Msx2* might regulated eye development through visual photo transduction pathway (Fig. 6D). Reactome enrichment analysis classified 18 genes (*Rcvrn*, *Gnat1*, *Rho*, *Gngt1*, *Pde6g*, *Sag*, *Pde6a*, *Guca1a*, *Guca1b*, *Slc24a1*, *Gucy2e*, *Grk1*, *Pde6b*, *Rgs9bp*, *Gucy2f*, *Rgs9*, *Gnb5*, *Gnb1*) into visual phototransduction category. There is no enough reference about the expression and function of these genes in lens. Future work is needed to clarify their expression and function in lens. Therefore, *Msx2* deficiency dramatically disturbed the gene expression profile of developing lens.

Dysregulated calcium signaling pathways after *Msx2* conditional deletion

Previous studies have demonstrated that a calcium signaling pathway is essential for lens development [23]. To verify the RNA-Seq analysis results, we performed qPCR to

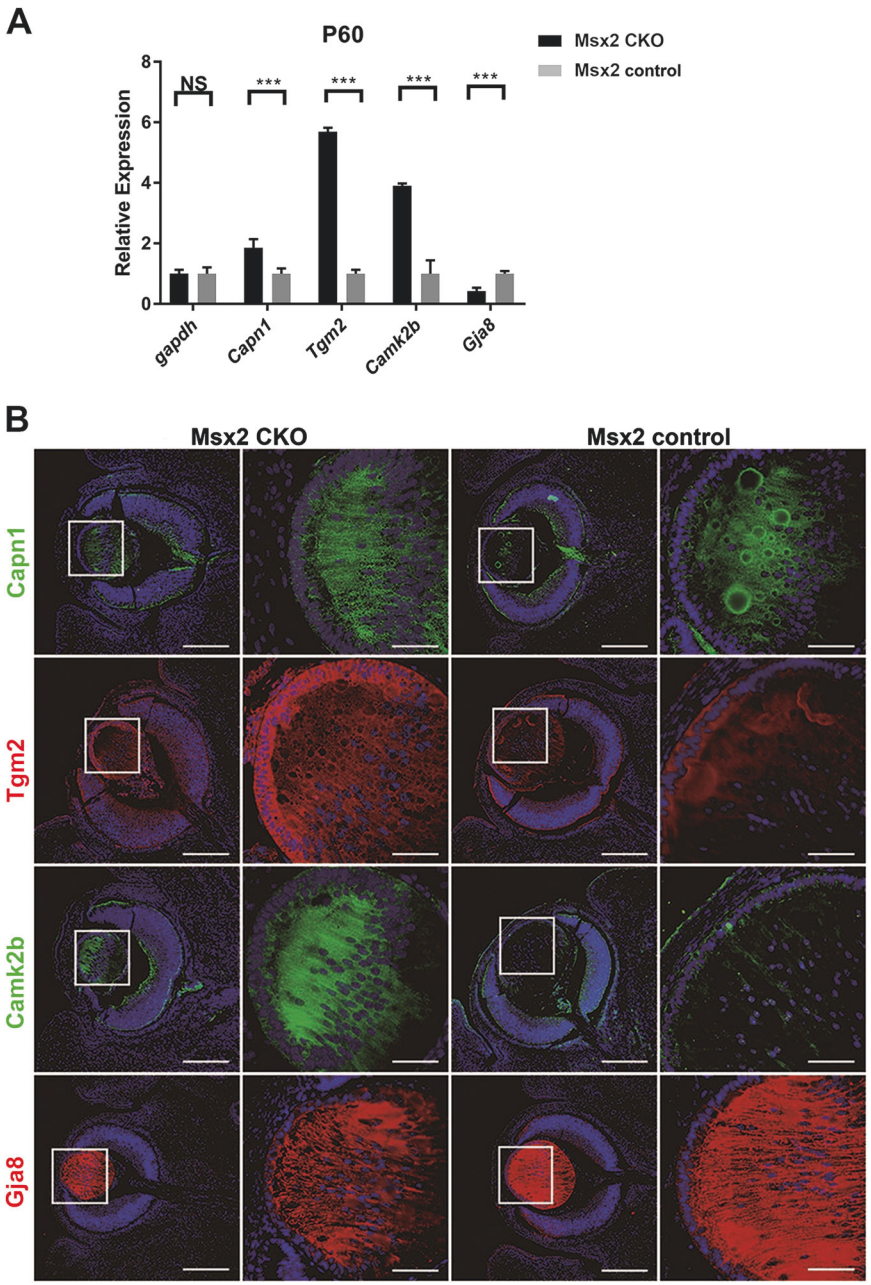

Fig. 7 Expression of Capn1, Tgm2, Camk2b, and Gja8 in *Msx2* CKO and *Msx2* control group lens. **A** qPCR detection of the mRNA expression of *Capn1*, *Tgm2*, and *Camk2b* are upregulated and *Gja8* is downregulated within *Msx2* CKO lens compare to the control group at P60. *gapdh* serves as loading control. *Msx2* CKO is normalized to *Msx2* control which is arbitrarily set as 1. Ten mice/20 eyes at P60 from each group were evaluated to compare gene expression; $N = 3$; $^{***}P < 0.0001$. **B** Immunohistochemistry analysis protein expression of Capn1, Tgm2, Camk2b are upregulated and Gja8 is downregulated in *Msx2* CKO lens compare to *Msx2* control mice at E14.5. Right panels show the enlarged view of the boxed regions in the left panels. Three mice/six eyes at E14.5 from each group were evaluated to compare protein expression; $N = 3$; E embryonic, P postnatal, Scale bars: 400 um, 200 um

determine the mRNA expression of Calpain 1 (*Capn1*), Transglutaminase 2 (*Tgm2*), calcium/calmodulin-dependent protein kinase 2b (*Camk2b*), and *Gja8* at P60 in lenses of *Msx2* CKO mice and *Msx2* control mice (Table 1). We found that *Capn1*, *Tgm2*, and *Camk2b* were significantly upregulated in *Msx2* CKO mice compared to control mice, and *Gja8* expression was significantly downregulated ($P < 0.01$) in *Msx2* CKO mice (Fig. 7A). These results were also verified by immunofluorescence assays of lenses from *Msx2* CKO and *Msx2* control lenses which were performed at E14.5. Capn1 expression slightly increased in differentiated lens cells from *Msx2* CKO mice. Tgm2 was expressed in all lens cells, and its expression increased in *Msx2* CKO mice at E14.5. Camk2b expression increased mainly in differentiated lens cells compared with *Msx2* control mice. However, Gja8 expressed at both lens epithelium cell and lens fiber cells, and its expression decreased in *Msx2* CKO mice (Fig. 7B). The above data indicate that *Msx2* is vital for a calcium signaling pathway in lens development.

Abnormal lens crystallins expression in *Msx2* conditional knockout mice

Among the dysregulated genes found by RNA-Seq in *Msx2* CKO mice, crystallin family members are notable because

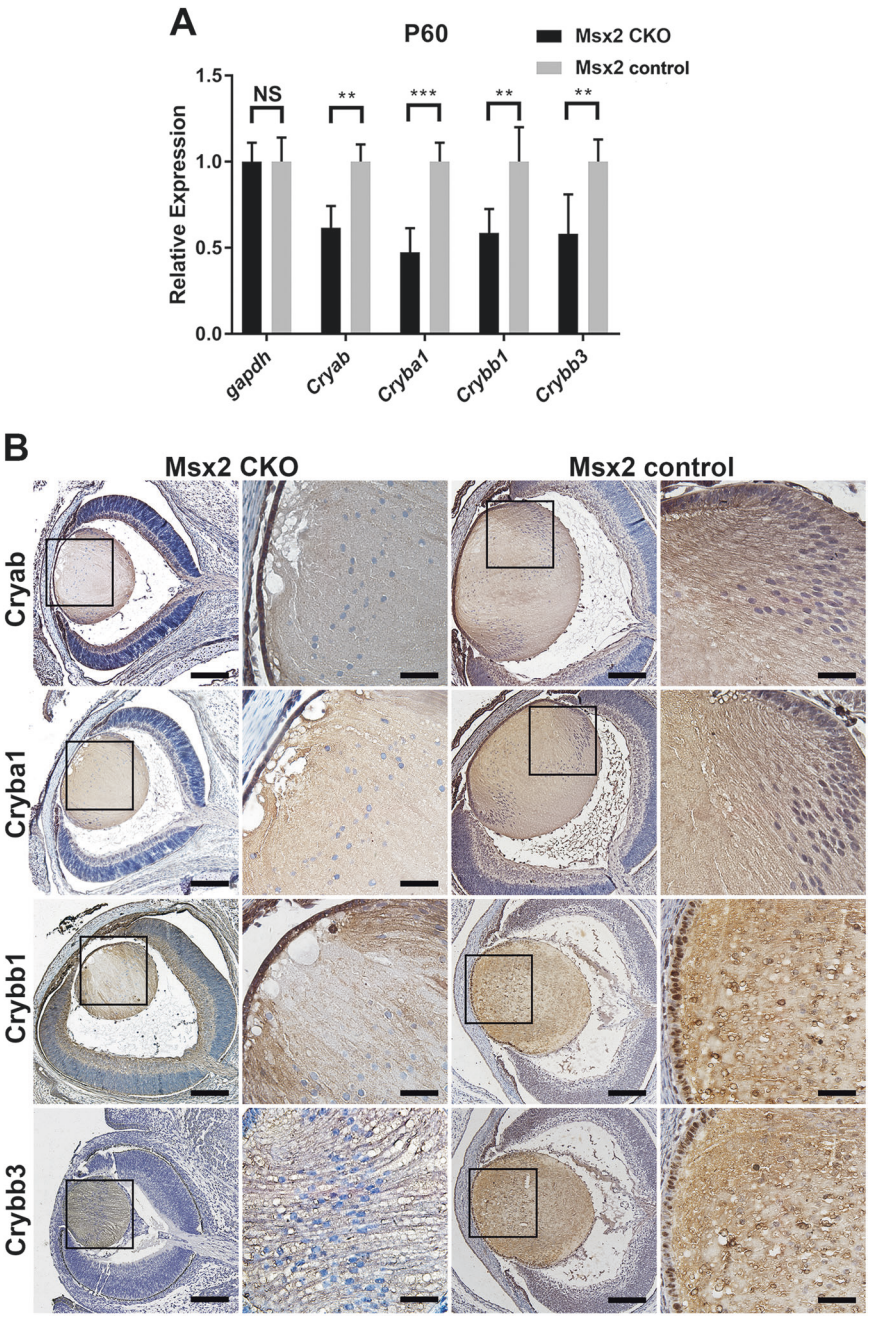

Fig. 8 Abnormal crystallin expression and defective lens architecture in *Msx2* CKO lens. **A** Relative expression of *Cryab*, *Cryba1*, *Crybb1* and *Crybb3* are downregulated in *Msx2* CKO compared to *Msx2* control lens at P60 as assessed by RT-qPCR. Ten mice/20 eyes at P60 from each group were evaluated to compare gene expression; $N = 3$; $^{**}P < 0.001$, $^{***}P < 0.0001$. **B** Cryab, Cryba1, Crybb1, and Crybb3 proteins in *Msx2* CKO and *Msx2* control lens at P60 are detected by immunohistochemistry. They are all downregulated in *Msx2* CKO mice lens fiber cells compare to the control group. Three mice/ six eyes at E14.5 from each group were evaluated to compare protein expression; $N = 3$; Scale bars: 400 um, 100 um

they are highly expressed during lens development. To verify the RNA-Seq analysis result mRNA level of crystallin ab (*Cryab*), crystallin ba1 (*Cryba1*), crystallin bb1 (*Crybb1*), and crystallin bb3 (*Crybb3*) were determined by RT-qPCR. As expected, all of them were downregulated in *Msx2* CKO mice (Fig. 8A). Consistently, downregulation of Cryab, Cryba1, Crybb1, and Crybb3 proteins were found throughout the whole lens of *Msx2* CKO mice (Fig. 8B). Since crystallin function as lens structure proteins, loss of crystallin affected lens structure and morphology.

Discussion

Msx2 plays an important role in multiple organ development [8, 24–29]. To investigate possible functions of *Msx2* in early ocular development, a precious study using transgenic mice overexpressing *Msx2* found that forced expression of the *Msx2* gene resulted in optic nerve aplasia and microphthalmia in all transgenic mice [13]. Marker analysis showed suppression of *Bmp4* and induction of *Bmp7* expression in the optic vesicle. In our previous study, germline knockout *Msx2* in mice led to microphthalmia or

anophthalmia, corneal and lens dysgenesis resembling Peters anomaly and microphthalmia can be seen in humans [14]. Lens vesicle growth and development were affected by *Msx2* traditional knockout mice. Moreover, loss of *Msx2* caused *FoxE3* and *Prox1* expression changes that further provided evidence of the important role of *Msx2* in regulating ocular development [14].

After the optic vesicle forms at E9.5, the neuroectoderm thickening in the lateral wall of the optic vesicle is destined to become the neural retina [13]. The corresponding surface ectodermal thickening becomes the lens placode. According to a previous study, *Msx2* gene expression was detected at optic vesicle and adjacent ectoderm at E9.5 [14]. Therefore, traditional knockout of *Msx2* gene perturbed lens and retina development simultaneously. As previous studies have shown, induction between lens vesicle and optic vesicle exists through the ocular development process [13, 14]. We could not distinguish whether dysregulated *Msx2* gene expression or abnormal lens-retina induction leads to lens dysgenesis in *Msx2* traditional knockout mice. Use of *Le-Cre* mice, which is under the control of the lens ectoderm promoter of *Pax6*, helped us eliminate the effect of abnormal retina development caused by lens-retina induction, and demonstrate lens development changes when a gene was conditionally deleted at the surface ectoderm.

In this study, using conditional *Msx2* knockout mice, we demonstrated that *Msx2* was a significant contributor to lens development. Without the *Msx2* gene in the surface ectoderm, mice were born with phenotypes consistent with ASD and congenital cataract. Compared with traditional *Msx2* knockout mice, *Msx2* CKO mice showed moderately abnormal phenotype during ocular development. The mouse eyes appeared moderately small, although all the ocular tissue was developed [14]. In addition, the corneal thickness decreased, and lens opacity and dysgenesis were observed. Moreover, we observed lens cell proliferation and apoptosis from E12.5. Compared with the control group, lens cell proliferation in *Msx2* CKO mice significantly decreased through the lens development process. A significantly higher apoptosis rate was seen in in *Msx2* CKO lens, consistent with the results found in conventional *Msx2* KO mice [14]. A previous study showed that germline knockout of *Msx2* may result in the persistent presence of lens stalk, due to increased proliferation rate in anterior lens epithelial cells after E14.5 [14]. However, lower cellular proliferation and ahigher apoptosis rate in the lens epithelial cells were found in *Msx2* CKO mice, which might explain why *Msx2* CKO mice did not develop lenses as small as those in the KO mice, and why the lens separated from the cornea at the appropriate developmental stage.

Further investigation into the complex interactions among *Msx2* and various transcriptional regulators and signaling molecules in ocular development may help clarify the pathogenesis of ASD. We conducted the RNA-seq analysis on P60 eyes in order to determine the detailed mechanism of *Msx2* conditional deletion in regulation of lens development. When we set the threshold at a 2-fold or greater change in expression of genes between *Msx2* CKO and *Msx2* control mice, 1911 DEGs were detected. Among them, 1586 genes were upregulated and the rest were downregulated. According to the RNA-seq results, calcium signaling pathway was one of the most dysregulated pathways in *Msx2* CKO mice. Previous studies showed that calcium controls lens cell homeostasis and lens development [30–32]. Intracellular calcium homeostasis requires normal cellular gap junctions [33–35]. *Gja8* (Cx50) and two alpha connexin family members, are expressed in ocular lens [36, 37]. *Gja8* is an important gap junction factor for lens development and is responsible for calcium coupling and regulating Ca^{2+} in lens fiber cell membranes. Substitution of aspartate-47 (D47) of *Gja8* has been linked to an autosomal dominant congenital cataract in several human pedigrees [38]. Smaller lenses and lens opacity were found in *Gja8* mutant mice [39, 40]. *Gja8* expression was downregulated when *Msx2* was conditionally deleted in mouse lens.

We also found that Capn1, Tgm2, Camk2b were upregulated in *Msx2* CKO lens, which maybe the results of increased calcium level in lens cells. Fodrin, filensin and Vimentin were known as substrates of calpain in lens [41, 42]. Calpain activation caused by intracellular calcium overloading was associated with several pathological conditions, including cataracts in animals [43]. Calpain-mediated proteolysis of crystallin may led to increased light scatter [44]. Moreover, alpha-crystallin, beta-crystallin, and vimentin can be cross-linked by Tgm2 when it is up-regulated [45, 46]. Tgm2 catalyzed dimerization of alpha-crystallin, which might be a key step of initiating protein aggregation.

Previous studies have shown that calmodulin (CAM) directly interacts with aquaporin 0 (AQP0) C-terminus in a calcium dependent manner to regulate water permeability of AQP0 [47, 48]. Another study identified a missense mutation (p.R233K) in the putative CAM binding domain of AQP0 C-terminus in a congenital cataract family [49]. Our results demonstrate that *Camk2b* was upregulated in *Msx2* CKO mice, and the *Camk2b* upregulation might lead to CAM hydrolysis and affect AQP0 indirectly.

The shortcoming of this study is that P60 lenses were selected for RNA-sequencing, but defects in lens development were observed as early as E10.5 in our previous study [15] and more prominently at birth. At different stages of lens development, gene regulation and expression varied and the results at P60 were dissimilar to those at E14.5 . While RNA-seq at P60 identifies interesting potential transcriptional changes in *Msx2* CKO lenses RNA-seq

performed at an earlier stage could closer to the onset of the phenotype which will reveal more direct downstream targets of *Msx2*. The purpose of RNA-sequencing in this study was to provide clues to figure out the possible gene downstream genes regulated by *Msx2* at early stage. Future research should include obtaining additional lens samples at earlier developmental stages.

In summary, the current work demonstrates that conditional deletion of *Msx2* gene at the surface ectoderm influenced lens cell proliferation and apoptosis, leading to ASD and lens opacity. We provide the first direct genetic evidence that *Msx2* gene influences lens development through a calcium signaling pathway. The results further support the importance of *Msx2* in eye development. This study provides important additional understanding of the *Msx2* gene function. In the future, we may recommend genetic testing of *Msx2* mutations for patients with a clinical diagnosis of ASD. Further studies in investigating interactions between calcium signaling pathway and *Msx2* may provide further insight into lens development.

Acknowledgements We are grateful to Dr. Yi-Hsin Liu (University of Southern California, Los Angeles) for experimental animal support. Funds for these studies were provided by the China Postdoctoral Science Foundation (2015M570517) and the Program of National Natural Science Foundation of China (No. 81371003; 81870646).

Compliance with ethical standards

Conflict of interest The authors declare that they have no conflict of interest.

Publisher's note: Springer Nature remains neutral with regard to jurisdictional claims in published maps and institutional affiliations.

References

1. Ito YA, Walter MA. Genomics and anterior segment dysgenesis: a review. Clin Exp Ophthalmol. 2014;42:13–24.
2. Gould DB, John SW. Anterior segment dysgenesis and the developmental glaucomas are complex traits. Hum Mol Genet. 2002;11:1185–93.
3. Reis LM, Semina EV. Genetics of anterior segment dysgenesis disorders. Curr Opin Ophthalmol. 2011;22:314–24.
4. Sowden JC. Molecular and developmental mechanisms of anterior segment dysgenesis. Eye. 2007;21:1310–8.
5. Trainor PA, Tam PP. Cranial paraxial mesoderm and neural crest cells of the mouse embryo: co-distribution in the craniofacial mesenchyme but distinct segregation in branchial arches. Development. 1995;121:2569–82.
6. Gage PJ, Rhoades W, Prucka SK, et al. Fate maps of neural crest and mesoderm in the mammalian eye. Invest Ophthalmol Vis Sci. 2005;46:4200–8.
7. Davidson D. The function and evolution of Msx genes: pointers and paradoxes. Trends Genet. 1995;11:405–11.
8. Elanko N. Functional haploinsufficiency of the human homeobox gene MSX2 causes defects in skull ossification. Nat Genet. 2000;24:387–90.
9. Kim B-K, Yoon SK. Hairless down-regulates expression of Msx2 and its related target genes in hair follicles. J Dermatol Sci. 2013;71:203–9.
10. Ramos C, Robert B. msh/Msx gene family in neural development. Trends Genet. 2005;21:624–32.
11. Babajko S, de La Dure-Molla M, Jedeon K, et al. MSX2 in ameloblast cell fate and activity. Front Physiol. 2014;5:510.
12. Chen YH, Ishii M, Sun J, et al. Msx1 and Msx2 regulate survival of secondary heart field precursors and post-migratory proliferation of cardiac neural crest in the outflow tract. Dev Biol. 2007;308:421–37.
13. Wu L-Y, Li M, Hinton DR, et al. Microphthalmia resulting fromMsx2-induced apoptosis in the optic vesicle. Invest Opthalmol Vis Sci. 2003;44:2404.
14. Zhao J, Kawai K, Wang H, et al. Loss of Msx2 function down-regulates the FoxE3 expression and results in anterior segment dysgenesis resembling Peters anomaly. Am J Pathol. 2012;180:2230–9.
15. Yu Z, Yu W, Liu J, et al. Lens-specific deletion of the Msx2 gene increased apoptosis by enhancing the caspase-3/caspase-8 signaling pathway. J Int Med Res. 2018;46:2843–55.
16. Bensoussan V, Lallemand Y, Moreau J, et al. Generation of an Msx2-GFP conditional null allele. Genesis. 2008;46:276–82.
17. Dorà NJ, Collinson JM, Hill RE, et al. Hemizygous Le-Cre transgenic mice have severe eye abnormalities on some genetic backgrounds in the absence of LoxP sites. PLoS One. 2014;9(10):e109193.
18. Ashery-Padan R. Pax6 activity in the lens primordium is required for lens formation and for correct placement of a single retina in the eye. Genes Dev. 2000;14:2701–11.
19. Pizard A, Haramis A, Carrasco AE, et al. Whole-mount in situ hybridization and detection of RNAs in vertebrate embryos and isolated organs. Curr Protoc Mol Biol. 2004;Chapter 14:Unit14 19.
20. Calkins MJ, Reddy PH. Assessment of newly synthesized mitochondrial DNA using BrdU labeling in primary neurons from Alzheimer's disease mice: Implications for impaired mitochondrial biogenesis and synaptic damage. Biochim Biophys Acta. 2011;1812:1182–9.
21. Andley UP, Tycksen E, Mcglasson-Naumann BN, et al. Probing the changes in gene expression due to α-crystallin mutations in mouse models of hereditary human cataract. PLoS One. 2018;13(1):e0190817.
22. Hoang TV, Kumar PK, Sutharzan S, et al. Comparative transcriptome analysis of epithelial and fiber cells in newborn mouse lenses with RNA sequencing. Mol Vis. 2014;20:1491–517.
23. Marko G, Rene M, Aleš F, et al. The analysis of intracellular and intercellular calcium signaling in human anterior lens capsule epithelial cells with regard to different types and stages of the cataract. PLoS One. 2015;10(12):e0143781.
24. Jabs EW, Muller U, Li X, et al. A mutation in the homeodomain of the human MSX2 gene in a family affected with autosomal dominant craniosynostosis. Cell. 1993;75:443–50.

25. Liu YH, Kundu R, Wu L, et al. Premature suture closure and ectopic cranial bone in mice expressing Msx2 transgenes in the developing skull. Proc Natl Acad Sci. 1995;92:6137–41.
26. Liu Y-H, Ma L, Kundu R, et al. Function of the Msx2 gene in the morphogenesis of the skulla. Ann N Y Acad Sci. 1996;785:48–58.
27. Liu YH, Tang Z, Kundu RK, et al. Msx2 gene dosage influences the number of proliferative osteogenic cells in growth centers of the developing murine skull: a possible mechanism for Msx2 -mediated craniosynostosis in humans. Dev Biol. 1999;205(2):260–74.
28. Jiang TX, Liu YH, Widelitz RB, et al. Epidermal dysplasia and abnormal hair follicles in transgenic mice overexpressing homeobox gene MSX-2. J Invest Dermatol. 1999;113:230–7.
29. Satokata I, Ma L, Ohshima H, et al. Msx2 deficiency in mice causes pleiotropic defects in bone growth and ectodermal organ formation. Nat Genet. 2000;24:391–5.
30. Duncan G, Bushell AR. Ion analyses of human cataractous lenses. Exp Eye Res. 1975;20:223–30.
31. Duncan G, Jacob TJC. Calcium and the physiology of cataract. Ciba Foundation Symposium 106–Human Cataract Formation. John Wiley & Sons, Ltd., UK: Cardiff University; 2008. p. 132–62.
32. Duncan G, Webb SF, Dawson AP, et al. Calcium regulation in tissue-cultured human and bovine lens epithelial cells. Invest Ophthalmol Vis Sci. 1993;34:2835.
33. Jiang JX. Gap junctions or hemichannel-dependent and independent roles of connexins in cataractogenesis and lens development. Curr Mol Med. 2010;10:851–63.
34. Gong X, Cheng C, Xia CH. Connexins in lens development and cataractogenesis. J Membr Biol. 2007;218:9–12.
35. Gao J, Sun X, Martinez-Wittinghan FJ, et al. Connections between connexins, calcium, and cataracts in the lens. J Gen Physiol. 2004;124:289–300.
36. Paul DL, Ebihara L, Takemoto LJ, et al. Connexin46, a novel lens gap junction protein, induces voltage-gated currents in nonjunctional plasma membrane of Xenopus oocytes. J Cell Biol. 1991;115:1077–89.
37. White TW, Bruzzone R, Goodenough DA, et al. Mouse Cx50, a functional member of the connexin family of gap junction proteins, is the lens fiber protein MP70. Mol Biol Cell. 1992;3:711–20.
38. Berthoud VM, Minogue PJ, Yu H, et al. Connexin50D47A decreases levels of fiber cell connexins and impairs lens fiber cell differentiation. Invest Ophthalmol Vis Sci. 2013;54:7614–22.
39. Hu S, Wang B, Zhou Z, et al. A novel mutation in Gja8 causing congenital cataract-microcornea syndrome in a Chinese pedigree. Mol Vis. 2010;16:1585.
40. Ming Y, Xiong C, Shui QY, et al. A novel connexin 50 (GJA8) mutation in a Chinese family with a dominant congenital pulverulent nuclear cataract. Mol Vis. 2008;14:418–24.
41. Roy D, Chiesa R, Spector A. Lens calcium activated proteinase: degradation of vimentin. Biochem Biophys Res Commun. 1983;116:204–9.
42. Sanderson J, Marcantonio JM, Duncan G. Calcium ionophore induced proteolysis and cataract: inhibition by cell permeable calpain antagonists. Biochem Biophys Res Commun. 1996;218:893–901.
43. Biswas S, Harris F, Dennison S, et al. Calpains: targets of cataract prevention? Trends Mol Med. 2004;10:78–84.
44. Shih M, David LL, Lampi KJ, et al. Proteolysis by m-calpain enhances in vitro light scattering by crystallins from human and bovine lenses. Curr Eye Res. 2001;22:458–69.
45. Shridas Preetha, Sharma Yogendra, Balasubramanian D. Transglutaminase-mediated cross-linking of α-crystallin: structural and functional consequences. FEBS Lett. 2001;499:245–50.
46. Shin DM, Jeon JH, Kim CW, et al. Cell type-specific activation of intracellular transglutaminase 2 by oxidative stress or ultraviolet irradiation: implications of transglutaminase 2 in age-related cataractogenesis. J Biol Chem. 2004;279:15032–9.
47. Gold MG, Reichow SL, O'Neill SE, et al. AKAP2 anchors PKA with aquaporin-0 to support ocular lens transparency. EMBO Mol Med. 2012;4:15–26.
48. Rose KM, Wang Z, Magrath GN, et al. Aquaporin 0-calmodulin interaction and the effect of aquaporin 0 phosphorylation. Biochemistry. 2008;47:339–47.
49. Hu S, Wang B, Qi Y, et al. The Arg233Lys AQP0 mutation disturbs aquaporin0-calmodulin interaction causing polymorphic congenital cataract. PLoS One. 2012;7:e37637.